Electronic Supplementary Material (ESI) for Journal of Materials Chemistry

Supplementary Information

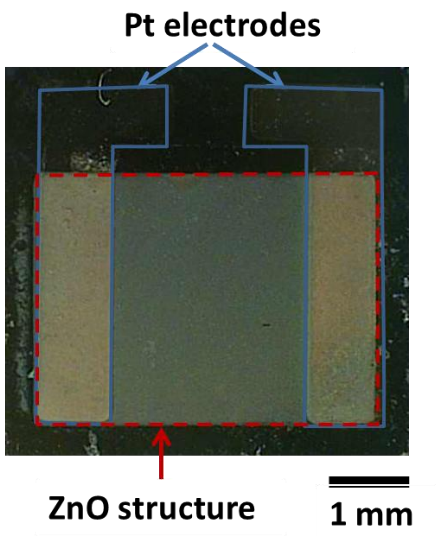

Fig. S1 Photograph of a sensor device.

Transmission electron microscopy (TEM) images of the nanorods obtained from different concentrations of 0.01, 0.04, and 0.05 M are shown in Fig. S2. A high-resolution TEM image (Fig. S2-d) shows that the nanorod was grown along the [0001] direction as determined by the interplanar spacing of 0.25 nm corresponding to the (0002) plane of hexagonal ZnO.

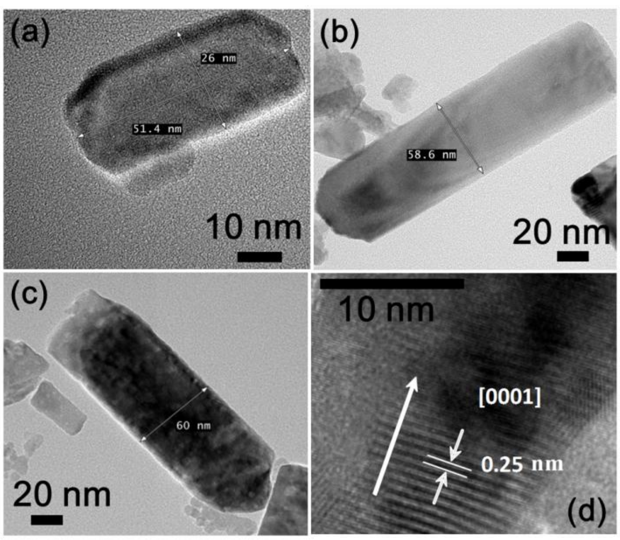

Fig. S2 TEM image of the nanorods in the ZnO-UL structures grown in (a) 0.01 M, (b) 0.04 M, and (c) 0.05 M solutions. (d) A high-resolution image for growth with 0.04 M solution.

Fig. S3 shows the x-ray diffraction (XRD) patterns obtained from ZnO-UL samples prepared from different solution concentrations. Apart from the Si(002) peak for the substrate, all the other peaks can be indexed to the hexagonal wurtzite structure of ZnO with lattice parameters of a = 3.25 Å and c = 5.21 Å, in good agreement with the standard XRD data for ZnO (JCPDS 36-1451). No diffraction peaks from impurities were observed. The intensity of peaks increased with the increase in the solution concentration because of the corresponding increase in the volume of nanorods. This confirms the scanning electron microscopy (SEM) observations.

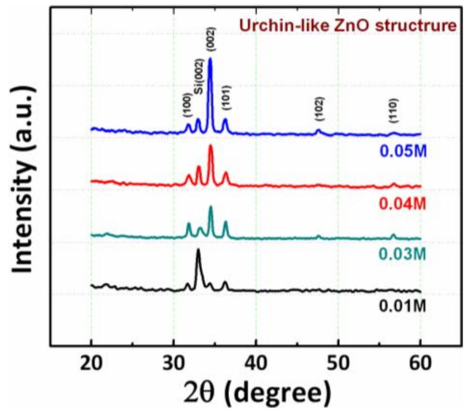

Fig. S3 XRD pattern of the hollow ZnO-UL structures grown for (a) 0.01 M, (b) 0.04 M, and (c) 0.05 M solutions.

The sensing responses of the urchin structures having short ZnO nanorods and long nanorods are compared. The simplest case is that the former has one short nanorod-to-nanorod current path [characterized by the resistance $r_a(2)$] and the latter has two current paths in parallel, one short nanorod and one long nanorod [characterized by the resistance $r_a(2)$ and $r_a(1)$, respectively], as illustrated in Fig. S4.

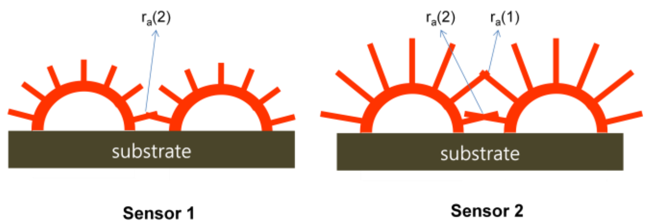

Fig. S4 The schematic urchin structure sensors having different nanorod lengths, and thus different number of parallel current paths.

The resistance of each path in air is given by

$$r_a(1) = 2r_a^{nr}(1) + r_a^c(1)$$
$$r_a(2) = 2r_a^{nr}(2) + r_a^c(2) \qquad \text{(e1)}$$

and the resistances upon exposure to NO gas are given by

$$r_g(1) = 2r_g^{nr}(1) + r_g^c(1)$$
$$r_g(2) = 2r_g^{nr}(2) + r_g^c(2) \qquad \text{(e2)}$$

Here we can assume that the nanorod diameters are all the same, and then the resistances at the nanorod-nanorod contacts due to energy barrier are also to be same for all the lengths of nanorods, or $r_a^c(1) = r_a^c(2) = r_a^c$ and $r_g^c(1) = r_g^c(2) = r_g^c$. Also note that $r_a(1) > r_a(2)$ due to the length difference in nanorods, and then we can put $r_a^{nr}(1) = \alpha\, r_a^{nr}(2)$ with the ratio of nanorod lengths α >1. Accordingly $r_g^{nr}(1) = \alpha\, r_g^{nr}(2)$.

Electronic Supplementary Material (ESI) for Journal of Materials Chemistry
This journal is © The Royal Society of Chemistry 2011

Now the responses of the sensors (S_1 for Sensor 1 and S_2 for Sensor 2) due to gas adsorption on the surface of the nanorods can be described by

$$S_1 = \frac{R_g - R_a}{R_a} = \frac{r_g(2)}{r_a(2)} - 1 \tag{e3}$$

$$S_2 = \frac{R_g - R_a}{R_a} = \frac{G_a - G_g}{G_g} = \frac{\dfrac{1}{r_a(1)} + \dfrac{1}{r_a(2)}}{\dfrac{1}{r_g(1)} + \dfrac{1}{r_g(2)}} - 1 = \frac{r_g(1) r_g(2)\{r_a(1) + r_a(2)\}}{r_a(1) r_a(2)\{r_g(1) + r_g(2)\}} - 1 \tag{e4}$$

Then

$$S_2 - S_1 = \frac{r_g(1) r_g(2)\{r_a(1) + r_a(2)\}}{r_a(1) r_a(2)\{r_g(1) + r_g(2)\}} - \frac{r_g(2)}{r_a(2)} = S_o\left[r_g(1) r_a(2) - r_a(1) r_g(2)\right] \tag{e5}$$

with

$$S_o = \frac{r_g(2)}{r_a(1) r_a(2)\{r_g(1) + r_g(2)\}} \tag{e6}$$

.

Now insert the Eqs. (e1) and (e2) to Eq. (e5) to obtain

$$\begin{aligned} S_2 - S_1 &= 2S_o\Big[2\{r_g^{nr}(1) r_a^{nr}(2) - r_a^{nr}(1) r_g^{nr}(2)\} \\ &\quad + r_a^c\{r_g^{nr}(1) - r_g^{nr}(2)\} - r_g^c\{r_a^{nr}(1) - r_a^{nr}(2)\}\Big] \\ &= 2S_o\Big[2\left(\alpha r_g^{nr}(2) r_a^{nr}(2) - \alpha r_a^{nr}(2) r_g^{nr}(2)\right) \\ &\quad + (\alpha - 1) r_a^{nr}(2) r_a^c\left(\frac{r_g^{nr}(2)}{r_a^{nr}(2)} - \frac{r_g^c}{r_a^c}\right)\Big] \end{aligned} \tag{e7}$$

(e6)

Since $S_2 > S_1$ from the experimental results (for example, the response of ZnO-UL-4 is larger than that of ZnO-UL-1), the term

$$f \equiv \frac{r_g^{nr}(2)}{r_a^{nr}(2)} - \frac{r_g^c}{r_a^c} \tag{e8}$$

$$f = \left(\frac{r_g^{nr}(2)}{r_a^{nr}(2)} - 1\right) - \left(\frac{r_g^c}{r_a^c} - 1\right) = \frac{\Delta r^{nr}(2)}{r_a^{nr}(2)} - \frac{\Delta r^c}{r_a^c} > 0 \tag{e9}$$

One finally obtains that the general inequality condition

$$\frac{\Delta r^{nr}(1)}{r_a^{nr}(1)} = \frac{\Delta r^{nr}(2)}{r_a^{nr}(2)} = ... = \frac{\Delta r^{nr}(i)}{r_a^{nr}(i)} = ... > \frac{\Delta r^c}{r_a^c} \tag{e10}$$